Advances in Understanding the Regulation of *acvrl1* Gene Expression

by

Thanhlong Gilbert Tran

BS, University of Maryland Baltimore County, 2014

Submitted to the Graduate Faculty of

the Department of Human Genetics

Graduate School of Public Health in partial fulfillment

of the requirements for the degree of

Master of Science

University of Pittsburgh

2019

UNIVERSITY OF PITTSBURGH

GRADUATE SCHOOL OF PUBLIC HEALTH

This thesis was presented

by

Thanhlong Gilbert Tran

It was defended on

June 4, 2019

and approved by

Yesim F. Demirci, MD, Associate Professor, Department of Human Genetics
Graduate School of Public Health, University of Pittsburgh

Mark J. Rebeiz, PhD, Associate Professor, Department of Biological Sciences
Kenneth P. Dietrich School of Arts and Sciences, University of Pittsburgh

Thesis Advisor:
Beth L. Roman, PhD, Associate Professor, Department of Human Genetics
Graduate School of Public Health, University of Pittsburgh

Beth L. Roman, PhD

Advances in Understanding the Regulation of *acvrl1* Gene Expression

Thanhlong Gilbert Tran, MS

University of Pittsburgh, 2019

Abstract

Hereditary hemorrhagic telangiectasia (HHT) is an autosomal dominant disease characterized by abnormal vascular structures known as telangiectases or arteriovenous malformations (AVMs). AVMs are direct connections between arteries and veins that may present as a tangle of abnormal, rupture-prone blood vessels, which can lead to hemorrhages, stroke, or high-output heart failure. HHT may be caused by haploinsufficiency due to the reduced levels of *acvrl1(*ALK1) or endoglin (ENG*)* on the endothelial cell surface, and it is well established that ALK1 signaling enhances *ENG* expression. Therefore, enhancing *ALK1* gene expression is a reasonable approach to the development of targeted therapeutics for HHT patients. In order to understand how the *alk1* gene is regulated, we generated a transgenic zebrafish model, *Tg(alk1e5:egfp)*^{pt517} , in which a 1910-bp DNA fragment from zebrafish *alk1* intron 1 in conjunction with a basal promoter drives EGFP expression. In this model, *egfp* expression is similar to endogenous *alk1,* with blood flow-dependent expression in select arteries, suggesting the presence of important regulatory elements within this intronic fragment. However, because this transgene inserted near an endothelial gene, the goal of my thesis work was to demonstrate a requirement for the *alk1* intron 1 element in driving the observed pattern of EGFP. To this end, I applied a genome editing technique, clustered regularly interspaced short palindromic repeat

(CRISPR)/Cas9, to delete this intronic element from *Tg(alk1e5:egfp)*^{pt517}. Using paired single guide RNAs, I successfully generated large deletions at the targeted site. To date, the largest deletion detected in F_1 offspring of P_0 founders was 1243 bp, eliminating the 5' end of the *alk1* intron 1 fragment. Current efforts are underway to characterize effects of deletions on the spatiotemporal pattern of EGFP expression. If complete deletion of this *alk1* intron 1 element eliminates arterial-specific and/or flow responsive transgene expression, future goals will be to identify specific cis-acting elements within this intron fragment that are responsible for this unique expression pattern. This work has public health significance because it is focused on validating a new model for understanding *ALK1* regulation, which may aid in development of targeted therapeutics for patients suffering from HHT, an understudied rare disease.

Table of Contents

List of Tables

List of Figures

Preface

I would like to thank my thesis chair and mentor, Dr. Beth L. Roman, for being such a wonderful guide throughout this journey. You had the patience to teach me what I needed to learn to get to this point. On so many levels, this effort would have been impossible without her. As I continue forward, I will strive to be as methodical and knowledgeable as Beth.

I would like to thank my thesis committee Dr. Yesim F. Demirci and Dr. Mark J. Rebeiz for dedicating their time and providing guidance through the research process.

Thank you to Dr. Xinyan Lu for spending her time guiding and working alongside me through this journey. Without her, my project would not have reached as far as its current state.

Likewise, thank you to the Dr. Roman lab, current and past members, for the constant support they have given me throughout my entire project. Special thanks to Teresa Capasso and Arulselvi Anbalagan for their expertise in zebrafish and technical support. Working among and laughing with these remarkable individuals was truly an amazing experience.

Last of all, I would like to thank my wonderful family, friends, and Michael for their unconditional love and support throughout the years, without you none of this would be possible.

1.0 Background

1.1 Hereditary Hemorrhagic Telangiectasia

Hereditary hemorrhagic telangiectasia (HHT) is an autosomal dominant vascular disorder with a prevalence of 1 in 5000 - 8000 individuals (Govani & Shovlin, 2009). HHT is characterized by abnormal vascular structures known as telangiectases or arteriovenous malformations (AVMs) (Govani & Shovlin, 2009). AVMs are direct connections between arteries and veins that may present as a tangle of abnormal, rupture-prone blood vessels that forms between arteries and veins (Whitehead, Smith, & Li, 2013). Arteries carry oxygen-enriched blood to the capillaries, where gas and nutrient exchange occur to the surrounding tissues. Then, the veins return oxygen-poor blood back to the heart and lungs. However, in the presence of an AVM, gas and nutrient exchange are impaired (Whitehead et al., 2013). In HHT patients, the most problematic AVMs are in the lung, brain, and liver.

Pulmonary arteriovenous malformations (PAVM) develop in 5 to 15 percent of HHT patients (Khurshid & Downie, 2002). PAVMs cause right-to-left shunts, resulting in poor blood oxygenation, profound dyspnea, fatigue, and cyanosis. PAVMs may also cause brain abscess and stroke due to failure to remove emboli and bacteria from the blood (White et al., 1988).

Cerebral arteriovenous malformations (CAVM) develop in 5 to 20 percent of HHT patients (Guttmacher, Marchuk, & White, 1995). Neurologic symptoms in HHT patients with CAVM include stroke, seizure, migraine, transient ischemic attack, and intracerebral and subarachnoid hemorrhage (Begbie, Wallace, & Shovlin, 2003; Willinsky, Lasjaunias, Terbrugge, & Burrows, 1990). Treatments for CAVMs include neurovascular surgery, embolotherapy, and stereotactic

radiosurgery. However, due to the possible risk a CAVM patient might experience, “a wait and see approach” is typically the initial action before recommending an invasive procedure.

Hepatic arteriovenous malformations (HAVMs) develop in about seventy-five percent of HHT patients. However, of these patients, only ten percent will develop clinically apparent symptoms. One of the most severe complications of HAVMs is high output heart failure (HOHF), caused by low systemic vascular resistance that leads to volume overload (Shovlin, 2015). Currently, the only treatment for HOHF in HHT patients is a liver transplant. However, recent studies suggest that AVMs may reform in transplanted livers (Felli et al., 2017).

Because HHT presents with variable age of onset and expressivity, and because clinicians are generally not very familiar with HHT, HHT is believed to be clinically underdiagnosed (Shovlin et al., 1994). However, the Curacao criteria can be applied to easily diagnose this disease. These criteria are: presence of epistaxis (frequent nose bleeds), telangiectases, visceral AVMs, and a family history of HHT (Shovlin et al., 1994). Individuals who display at least three of these four criteria have HHT, and individuals who display two of these criteria are characterized as suspected HHT patients.

1.2 Locus heterogeneity of HHT

There are three classifications of HHT, each of which is caused by mutations in genes that function in the transforming growth factor beta (TGFβ) superfamily signaling pathways. The two major genes that are responsible for HHT are activin receptor type 2 like 1 (*ALK1* or *ACVRL1)*, which encodes a transmembrane type I receptor serine/threonine kinase, and endoglin (*ENG)*, which encodes a non-signaling co-receptor. Mutations in these genes cause HHT2 and HHT1,

respectively, which together account for about 85-96% of disease (McDonald & Pyeritz, 1993). Mutations in *SMAD4,* which encodes a downstream signaling effector, cause HHT-juvenile polyposis syndrome (Gallione et al., 2004). More recently, several individuals with HHT-like phenotypes have been identified with mutations in *BMP9* (*GDF2*) (Wooderchak-Donahue et al., 2013), which encodes an ALK1 ligand.

1.3 BMP 9/10 Signaling Pathway

BMP9 and BMP10 are ligands that are responsible for the signaling pathway for HHT (David, Mallet, Mazerbourg, Feige, & Bailly, 2007). The BMP9 ligand is synthesized by the liver. The BMP10 ligand is predominantly synthesized by the heart but is also synthesized by the liver (Tillet et al., 2018). Both ligands are detected in circulation. These ligand dimers will trigger receptor complex formation and allow a type II receptor to phosphorylate a type I receptor, which phosphorylates receptor-specific (R-) SMAD 1, 5, or 8. The phosphorylated R-SMAD binds to SMAD4 and the complex translocates into the nucleus where it binds to and regulates expression of target genes (Ruiz-Llorente et al., 2017) (Figure 1).

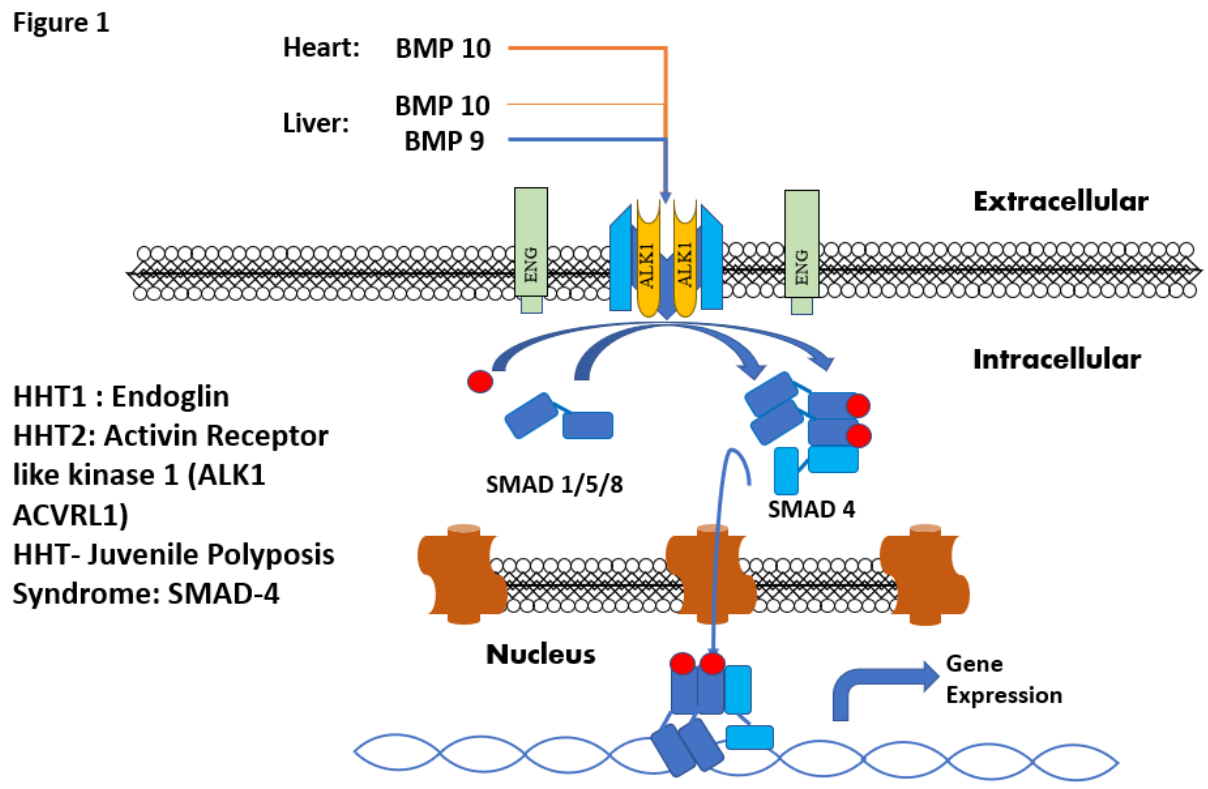

Figure 1 BMP9/BMP10 Signaling Pathway

BMP9/10 bind to a heterotetrameric complex composed of type I receptors (ALK1) and type II receptors. These ligand dimers will trigger receptor complex formation and allow a type II receptor to phosphorylate a type I receptor, which phosphorylates receptor-specific SMAD 1, 5, or 8. The phosphorylated R-SMAD binds to SMAD4 and the complex translocates into the nucleus where it binds to and regulates expression of target genes.

1.4 HHT Mechanism of Disease

In HHT, mutations occur throughout all exons of both *ALK1* and *ENG* and include missense mutations, nonsense mutations, insertions, and deletions. Most alleles are thought to be functional nulls. As such, HHT may be caused by haploinsufficiency due to the reduced levels of ALK1 or endoglin on the endothelial cell surface. Additionally, it is well established that ALK1

signaling enhances *ENG* expression (Tual-Chalot et al., 2014). Therefore, enhancing *ALK1* gene expression may be a reasonable approach to treating HHT1 and HHT2 patients. However, the possibility remains that HHT is caused by somatic second hits that eliminate functional protein (Roman & Hinck, 2017). If this is the case, then enhancing *ALK1* expression may not be helpful in HHT2 patients but may still be helpful in HHT1 patients because ENG enhances but is not required for ALK1 signaling (Ruiz-Llorente et al., 2017).

1.5 Regulation of Alk1 Gene Expression

Embryonically, *ALK1* is expressed predominantly in arterial endothelial cells closest to the heart, and expression requires blood flow (Corti et al., 2011). However, little is known regarding the regulatory elements that control this unique pattern of gene expression. Human *ALK1* expression is enhanced by Kruppel-like factor 6 (KLF6) and Sp1 (Garrido-Martin et al., 2013) via *cis* elements in the promoter. A genomic fragment spanning 9.2 kb of the mouse *Alk1* gene, which includes 2.7 kb of the promotor through intron 2, is sufficient to drive arterial-specific *Alk1* expression (Seki, Hong, Yun, Kim, & Oh, 2004). Following up on this discovery, Seki identified an evolutionarily conserved region within the 3' end of mouse *Alk1* intron 2 and human *ALK1* intron 1, and showed that this region, along with the promoter, was sufficient to drive arterial expression in a pattern similar to endogenous *Alk1* (Li, Yonenaga, & Seki, 2009; Seki et al., 2004). However, specific transcriptional regulatory mechanisms that drive the unique spatiotemporal pattern of *Alk1* expression have not been defined.

1.6 Zebrafish models of HHT

1.6.1 Zebrafish as a model for human development and disease

Zebrafish are a useful animal model for the study of normal and pathological vascular development. Since zebrafish lay hundreds of eggs, fertilization is external, and embryos are transparent, we can easily observe embryonic development and perform manipulations to modify gene expression and generate stable transgenic lines. In addition, transparency allows real-time imaging of vessel development in transgenic animals that express fluorescent proteins in their endothelial cells. Moreover, zebrafish have a stereotypical vertebrate body plan and share most of the same genes as humans: 71.4% of human genes have at least one zebrafish orthologue, while 69% of zebrafish genes have at least one human orthologue (Howe et al., 2013). Therefore, zebrafish are an important model for understanding how genes function in human health and disease.

1.6.2 Zebrafish models of HHT2

The function of ALK1 is conserved from humans to zebrafish. In the presence of blood flow, *alk1* is expressed in the arteries most proximal to the heart: first arch artery (AA1), internal carotid artery (ICA), caudal division of the internal carotid artery (CaDI), basal communicating artery (BCA), lateral dorsal aortae (LDA), and dorsal aorta (DA) (Roman et al., 2002). In the absence of *alk1*, zebrafish embryos develop cranial AVMs that connect the BCA or downstream basilar artery to neighboring veins. *alk1*-dependent vessels become enlarged in *alk1* mutants and AVMs develop downstream of these enlarged vessels, likely in response to altered hemodynamic

force (Rochon, Menon, & Roman, 2016). Moreover, the ALK1 signaling pathway is conserved between zebrafish, mouse, and human: ligands Bmp9 and Bmp10 bind to endothelial *Alk1* and activate phosphorylation of Smad1/5/8 (Laux et al., 2013). These data validate zebrafish as a model for probing *alk1* transcriptional regulation and function in arterial endothelial cells.

1.6.3 Transgenic reporter of *alk1* expression

As mentioned earlier, a fragment spanning 9.2 kb of the mouse *Alk1* gene, including 2.7 kb of the promotor through intron 2, is sufficient to drive arterial-specific *Alk1* expression in mouse (Seki et al., 2004). Capitalizing on this knowledge, we generated a transgenic zebrafish model, *Tg(alk1e5:egfp)*^{pt517} , in which a 1910-bp DNA fragment from zebrafish *alk1* intron 1 (equivalent to mouse *Alk1* intron 2) is inserted upstream of a basal promoter that drives EGFP expression (Figure 2; B. Roman, unpublished). Our transgenic model expresses EGFP in a pattern that is very similar to endogenous *alk1*, with predominant expression in AA1, LDA, ICA, CaDI, and BCA. The only difference between *alk1* and *egfp* expression is precocious *egfp* in AA 3-5 (Figure 3). However, the transgene insertion site is in chromosome 20 within intron 6 of the 7-exon *pinx1* gene, just upstream of *sox7*, a gene that is expressed in endothelial cells (Figure 2). Others in the lab have demonstrated that *egfp* is restricted to *alk1*-positive ECs, whereas *sox7* is more widely expressed in arteries and in veins and *pinx1* is non-endothelial (Figure 3). However, to definitively demonstrate that the *alk1* intron 1 element is responsible for the distinct *egfp* expression pattern and is thus a true reporter of *alk1* expression, the goal of my thesis work is to demonstrate that this element is required for the observed pattern of EGFP expression.

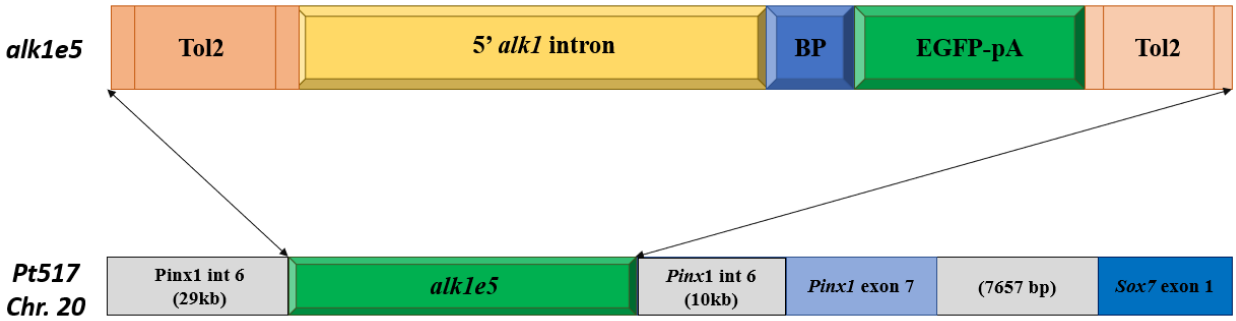

Figure 2 *alk1e5*: egfp insert location within transgenic line pt517

The *alk*1e5:egfp transgene inserted in *pinx1* intron 6, upstream of *sox7*.

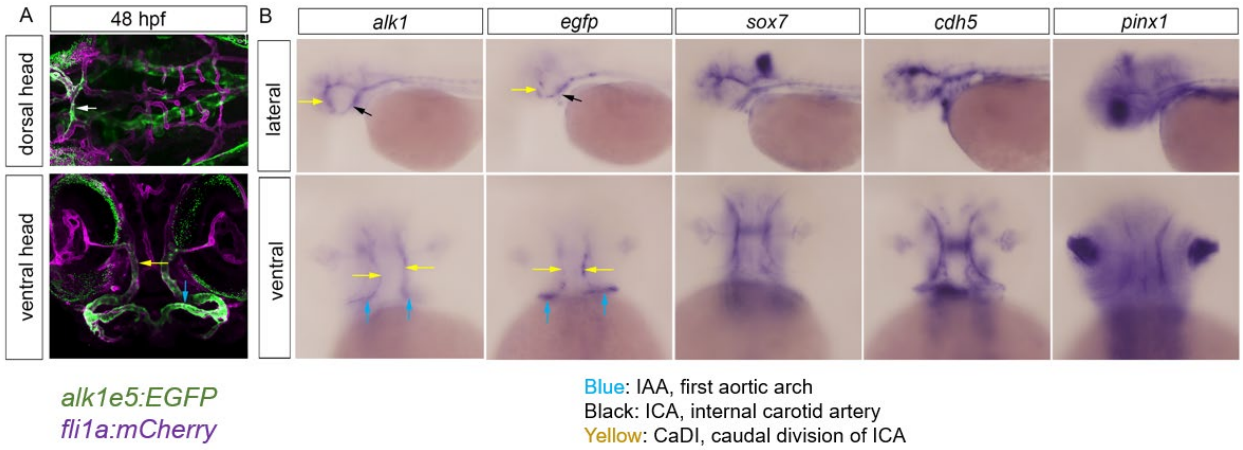

Figure 3 Tg (*alk1*e5:egfp) recapitulates endogenous alk1 expression

A) 2D confocal projection. *alk1*e5:EGFP expression is shown in green, all endothelial cells are magenta. B) In situ hybridization for indicated genes at 48 hpf, lateral (top) and ventral (bottom) views. Confocal images provided by B. Roman; in situ hybridization provided by X. Lu.

1.7 CRISPR/CAS9 Technique

To validate the *alk1* regulatory element that drives flow dependent, arterial EGFP expression in our transgenic zebrafish line, I applied a genome editing technique, clustered regularly interspaced short palindromic repeat (CRISPR)/Cas9. CRISPR is a natural defensive mechanism that evolved in certain bacteria and archaea that allows them to respond to foreign genetic material from viruses (Liu et al., 2017). In genome editing, single guide RNAs (sgRNAs) are designed that contain 20-23 nucleotides of sequence complementary to a target site in a gene of interest, and a transactivating RNA (trRNA) that binds Cas9 nuclease. The only constraint for targeting is a requirement for a protospacer adjacent motif (PAM), NGG, located immediately 3' to the sgRNA recognition site. The Cas9 nuclease is guided to the DNA by the sgRNA and will create a double strand break (DSB). DSBs typically repair through non-homologous end joining (NHEJ), causing deletions and insertions that may lead to frameshift-mediated gene disruption (Campenhout et al., 2019). Generating two double strand breaks flanking a region of interest will result in deletion of the intervening sequence (Liu et al., 2017). However, sgRNA efficiency varies, and there is considerable risk of causing mutation in off-target sites (Campenhout et al., 2019).

1.8 Objectives/Specific Aims

With the aid of CRISPR, the goal of my thesis work was to validate that the *alk1* first intron fragment within our transgenic zebrafish model is responsible for the *alk1*-like expression of

EGFP, and to set the stage for the identification of subregions that may function as transcriptional enhancers or repressors.

Specific Aim 1: Identify sgRNAs that efficiently cut the *alk1e5:EGFP* transgene at sites that flank the *alk1* intron 1 fragment. I injected multiple guide RNAs (sgRNA) to guide the Cas9 protein to the sites flanking the *alk1* intron 1 fragment and tested DSB efficiency via PCR. I validated one 5' gRNA and one 3' sgRNAs that generated DSBs that were repaired by non-homologous end-joining.

Specific Aim 2: Delete large regions of *alk1* intron 1 in *Tg(alk1e5:egfp)* and determine whether this element is required to drive transgene expression in the observed *alk1*-like spatiotemporal pattern. I co-injected pairs of effective sgRNAs and assessed EGFP expression via fluorescence microscopy and deletion efficiency by PCR and sequencing. I validated the presence of large deletions in P0 embryos, identified P0 founders, and generated F1 lines. Analysis of the F1 lines is in progress.

2.0 Material and Methods

2.1 Fish Husbandry

Zebrafish were maintained according to standard protocol and used in experiments approved by Institutional Animal Care and Use Committee of University of Pittsburgh. Embryos were grown at 28.5°C in 30% Danieau [17 mM NaCl, 2 mM KCl, 0.12 mM $MgSO_4$, 1.8 mM Ca $(NO_3)_2$, 1.5 mM HEPES]. For imaging, embryo medium was supplemented with 0.003% phenylthiourea (Sigma) at ~8 hpf to prevent melanin synthesis.

2.2 sgRNA and Cas9 mRNA synthesis

CRISPR target sites were identified using Crispor, http://crispor.tefor.net/. The templates for *in vitro* transcription of sgRNAs were produced by PCR using oligonucleotides listed in Table 1. The PCR was conducted according to Bassett (Bassett & Liu, 2014). PCR Program: 98C, 30s; 98C, 10s; 60C, 30s; 72C, 15s; 35 cycles; 72C, 10 min; 4C, hold. The *in vitro* transcription was performed using MegaScript T7 Kit (Thermo Fisher, Waltham, MA USA). The RNA was purified using MegaClear Transcription Clean-Up (Thermo Fisher). Cas9 mRNA was synthesized from plasmid Cas9 MLM3613 (Addgene, Watertown, Massachusetts, USA #42251) using mMessage mMachine T7 Ultra (Ambion, Foster City, CA USA) and purified by phenol chloroform extraction/ammonium acetate precipitation. Alternatively, I used NLS-*Cas9* Protein (PNA Bio, #CP01-200).

Table 1 Oligonucleotides for sgRNA synthesis

Oligo Name	Oligo Sequence
5' target sites*	
1278 alk1e5 sgRNA	GAAATTAATACGACTCACTATAGGTATTGCGGTCTTTAATCCCGTTTTAGAGCTAG
1279 alk1e5 sgRNA	GAAATTAATACGACTCACTATAGGTGAGAACTTCTAGTGTCCAGTTTTAGAGCTAG
1280 alk1e5 sgRNA	GAAATTAATACGACTCACTATAGGCCAGATGGGCCCTCGAGCGTTTTAGAGCTAG
3' target sites	
1281 alk1e5 sgRNA	GAAATTAATACGACTCACTATAGGGTGCTTACGAATACACTGGTTTTAGAGCTAG
1282 alk1e5 sgRNA	GAAATTAATACGACTCACTATAGGTCTTTATTTCTAAGCTGCCGTTTTAGAGCTAG
Common primer	
	AAAAGCACCGACTCGGTGCCACTTTTTCAAGTTGATAACGGACTAGCCTTATTTTAA CTTGCTATTTCTAGCTCTAAAAC

*5' target sites are upstream of the *alk1e5* insert, while the 3' target sites are downstream of the insert. The 5' end of each oligo is encoding the T7 polymerase binding site; red lettering indicates sequence complementary to target site; and 3' end is a common oligonucleotide that base pairs with the common primer.

Table 2 Primer Sequences

Oligo Name	Oligo Sequence
Forward Primers	
994	ATATCCGTTCTACAAATAATCACAACTT
656	CAATCCTGCAGTGCTGAAAAGCCTC
1284	GGCGTTATTGCAAGCCATGT
1286	AGTCCTGAGAAAGTGCACTGT
Reverse Primers	
916	CTTTCACTTGAGTAAAATTTTTG
424	ACAAGAGCAATTGCAGAGAGA
1285	TCAGCTGCTCACAATAGCCT
545	CTGGGTCACATTTAAGACGG

2.3 Injection and genotyping

I generated embryos by outcrossing hemizygous *Tg(alk1e5:EGFP)*^{pt517} fish to wild types and injected one to four-cell stage embryos with ~2-3 nl of a solution containing 800 ng/µl *Cas9* mRNA, 25 ng/µl sgRNAs, and 6 µl phenol red dye (0.2M KCl, 0.5% Phenol Red). Alternatively, embryos were injected with ~2-3 nl of a solution containing 0.5 µg/µl NLS-*Cas9* Protein [PNA Bio, #CP01-200], 25 ng/µl individual sgRNAs, or 12.5 ng/µl 5' sgRNA plus 12.5 ng/µl 3' sgRNA with phenol red dye.

2.3.1 Validation of a single sgRNA efficiency

For PCR amplification of the targeted region, 3 dpf larvae were digested for 12 h at 50°C (10 mM Tris HCl, pH 8.0; 50 mM KCl; 0.3% Tween-20; 0.3% Nonidet P-40 Sub.; 0.5 mg/mL 20 mg/mL Proteinase K) and enzyme was deactivated for 10 min at 98°C. Samples were stored at -20°C. One µl of the solution was used as template in a standard 10 µl PCR (w/ AmpliTaq Gold (ThermoFisher): 94C, 10 min; 94C, 30s; 52C, 30s; 72C, 60s; 35 cycles; 72C, 7 min; 4C, hold) with primers listed in Table 2. Restriction enzymes that cut the wild type genomic DNA (gDNA) near the target site were then used to digest the PCR product (2 hrs) to identify embryos harboring mutations at the targeted site: while PCR products from wild type *Tg(alk1e5:egfp)* DNA contain the restriction site, DNA effectively targeted by CRISPR/Cas9 should not (Table 3). Representative PCR products were sequenced to verify deletion.

Table 3 PCR/Restriction Enzyme Assays for Testing sgRNAs

Oligo Name	Forward Primer	Reverse Primer	Restriction Enzyme	Expected Cut Fragments (wild type)		Expected Uncut Fragments (mutation)	Incubation Temperature	Incubation Time (hrs)
5' target sites								
1278 alk1e5 sgRNA	994	916	BstN1	130	123	253	60	2
1279 alk1e5 sgRNA	994	916	BstN1	132	121	253	60	2
1280 alk1e5 sgRNA	656	424	XhoI	137	135	272	37	2
3' target sites								
1281 alk1e5 sgRNA	1284	1285	DdeI	148	159	307	37	2
1282 alk1e5 sgRNA	1286	545	BstN1	162	87	249	60	2

2.3.2 Validation of deletion after co-injection two sgRNA

For PCR amplification of the targeted region, 3 dpf larvae were digested for 12 h at 50°C (10 mM Tris HCl, pH 8.0; 50 mM KCl; 0.3% Tween-20; 0.3% Nonidet P-40 Sub.; 0.5 mg/mL 20 mg/mL Proteinase K) and enzyme was deactivated for 10 min at 98°C. Samples were stored at -20°C. One µl of the solution was used as template in a standard 10 µl PCR (w/ Phusion Hot Start ii DNA Polymerase (ThermoFisher): 98C, 180s; 98C, 30s; 65C, 20s; 72C, 90s; 35 cycles; 72C, 10 min; 4C, hold) with designated primers listed in Table 4. To confirm the evidence of NHEJ, prior to sending our PCR samples for sequencing, we used ExoSAP-IT (ThermoFisher) to remove any excess primers. Representative PCR products were sequenced to verify deletion; when gel purification was necessary prior to sequencing, Qiagen gel purification kit (Qiagen, Germantown, Maryland, USA) was used.

Table 4 PCR Assays for Testing Coinjected sgRNAs

Oligo Name	Forward Primer	Reverse Primer	Expected Full Length PCR Product	Expected Complete Removal
1280/1281 alk1e5 sgRNA	656	1285	1615	280
1280/1282 alk1e5 sgRNA	656	545	2123	190

2.4 Fluorescent Imaging

An MVX-10 MacroView microscope with DP71 camera (Olympus America, Center Valley, PA, USA) was used to assess transgene expression in individual embryos at 3 dpf. Embryos were treated with tricaine (to impair movement) in 30% Danieau/0.003% phenylthiourea (PTU) (to prevent pigmentation) and scored as normal EGFP, no EGFP, or altered EGFP (increased, decreased, ectopic). Images were compiled with Adobe Photoshop CS2 version 9.0.2 (Adobe Systems, San Jose, CA, USA).

3.0 Results

3.1 Specific Aim 1: Identify sgRNAs that efficiently cut the intronic alk1 fragment within the alk1e5:EGFP transgene

3.1.1 Validation of sgRNA efficiency assays

My goal was to use CRISPR/Cas9 to generate DSBs flanking the *alk1* intron 1 fragment in *Tg(alk1e5:egfp)*^{pt517} zebrafish, thereby deleting this fragment, and assessing its requirement for transgene expression. After designing sgRNAs and corresponding efficiency assays (Tables 1,3), my next step was to validate these assays to confirm expected outcomes (Table 3) in uninjected *Tg(alk1e5:egfp)*^{pt517} DNA. Figure 4 shows that assays for sgRNAs 1278/1279, 1280, 1281, and 1282 performed as expected.

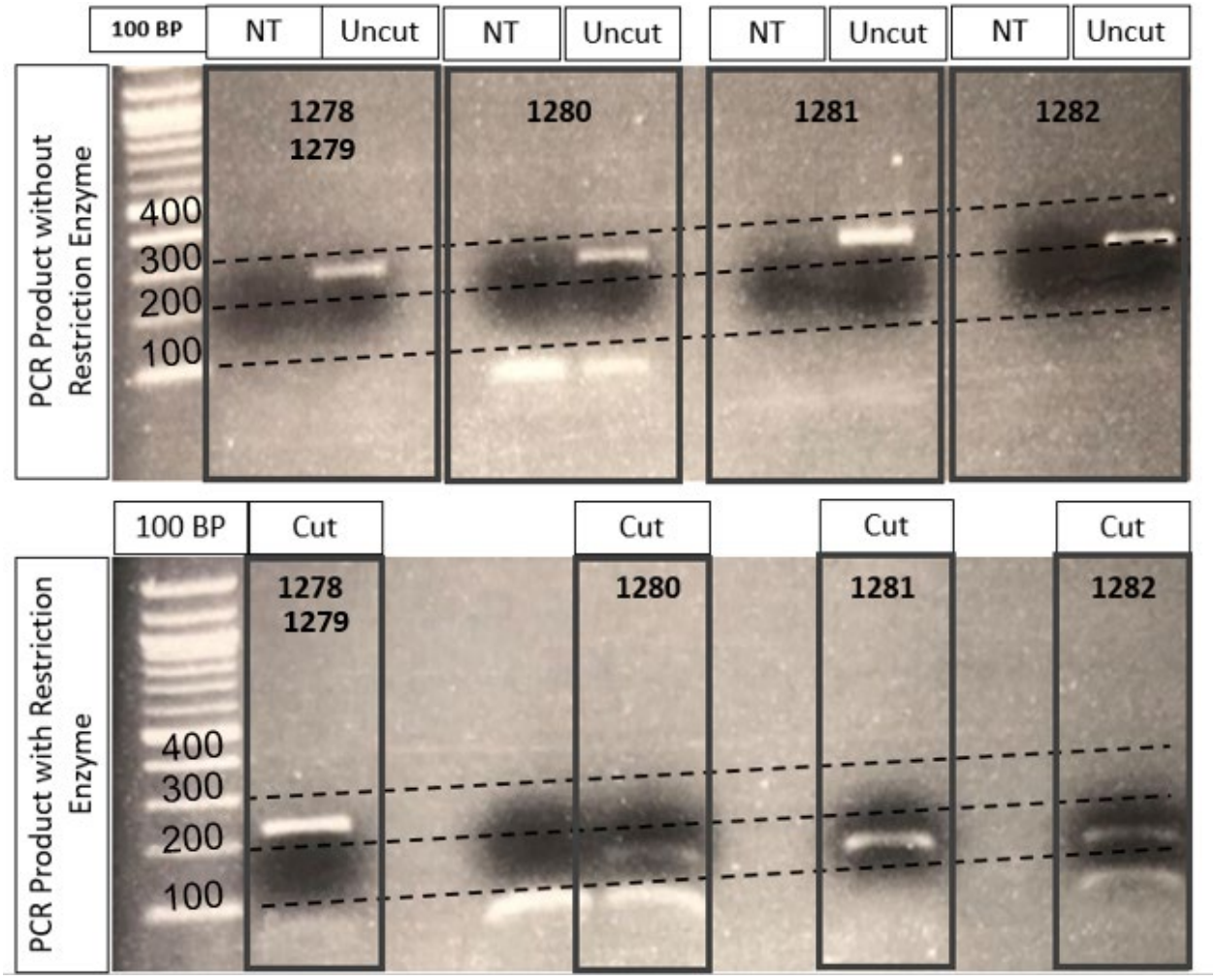

Figure 4 Validation of sgRNA efficiency assays

Top image shows PCR product generated from control pt517 embryos, validating expected band sizes (Table 2). Bottom image shows restriction enzyme-digested PCR products, validating expected band sizes (Table 2). Dotted lines, references for 300 bp, 200 bp, and 100 bp markers. NT, no template control.

3.1.2 Testing individual sgRNAs

Next, I applied these assays to pooled gDNA (5 µl/embryo, up to 24 embryos/pool, pooled based on scored EGFP) from sgRNA-injected embryos. In these samples, I expected to see only

an uncut band if the sgRNA was 100% efficient (cut all DNA in all embryos), or more likely, the uncut band plus the bands resulting from digest of the wild type gDNA. The presence of an uncut band demonstrates that one or more individual embryos had a DSB at the sgRNA target site. When an uncut band was present within the pooled gDNA from injected embryos, I repeated the assay on individual genomic DNA samples from the pool to gauge efficiency. Cutting efficiency was expressed as the number of individual embryos with an uncut band over the total number of samples assayed. My goal was to identify at least one sgRNA on each side of the intronic fragment that resulted in ≥ 50% efficiency on a per-embryo basis.

3.1.2.1 Targeting the 5' end of the alk1e5 transgene

Although I was not able to validate efficiency of gRNAs 1278 and 1279, I did validate sgRNA 1280. sgRNA 1280 targeted the 5' end of the *alk1e5* transgene, within the Tol2 transposon arm of the plasmid backbone (Figure 5a), with no target in the zebrafish genome. Using the validated sgRNA 1280 efficiency assay, pooled sgRNA-injected embryos showed some evidence of an uncut band, suggesting DSB and NHEJ that disrupted the restriction site (data not shown). The cutting efficiency for sgRNA 1280 was 13/20 embryos (65%) in the injected transgenic group (Figure 5b). I re-analyzed by PCR and sequencing a single gDNA sample that had shown evidence of deletion. The presence of double peaks 3' to the target site confirmed the presence of mosaic deletions (Figure 5c).

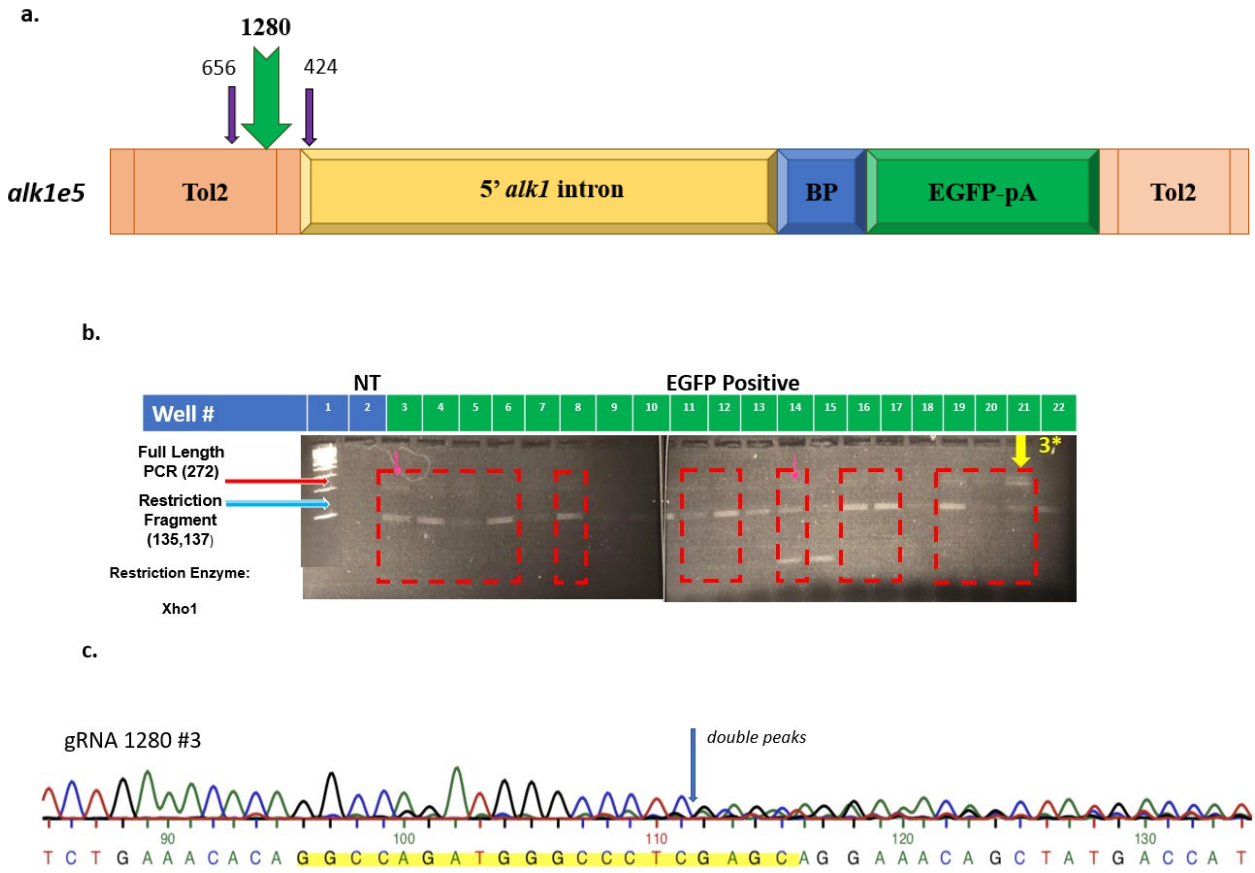

Figure 5 Validation of sgRNA 1280

a) sgRNA target site and PCR primer (656, 424) binding sites for efficiency assays for sgRNA 1280. b) Efficiency assay, individual embryos from EGFP-positive pool. Red dashed boxes represent samples showing evidence of mutation: 3* represents the PCR product chosen for sequencing. c) Sequence of PCR product showing double peaks 3' to the target sequence (yellow highlighting) of sgRNA 1280.

3.1.2.2 Targeting the 3' end of the alk1e5 transgene

sgRNA 1281 targeted the 3' end of the *alk1e5* transgene, within *alk1* intron 1, 5' to the basal promoter (Figure 6a). Using the validated sgRNA 1281 efficiency assay, pooled sgRNA-injected embryos showed some evidence of an uncut band, suggesting DSB and NHEJ that disrupted the restriction site (data not shown). I then tested individual embryos to calculate cutting

efficiency. The cutting efficiency for sgRNA 1281 was 13/20 embryos in the EGFP-positive group and 15/20 embryos in the EGFP-negative group; thus, the average cutting efficiency was 70% (Figure 6b, c). I re-analyzed by PCR and sequencing two gDNA samples that had shown evidence of deletion. The presence of double peaks 3' to the target site confirmed the presence of mosaic deletions (Figure 6b, c).

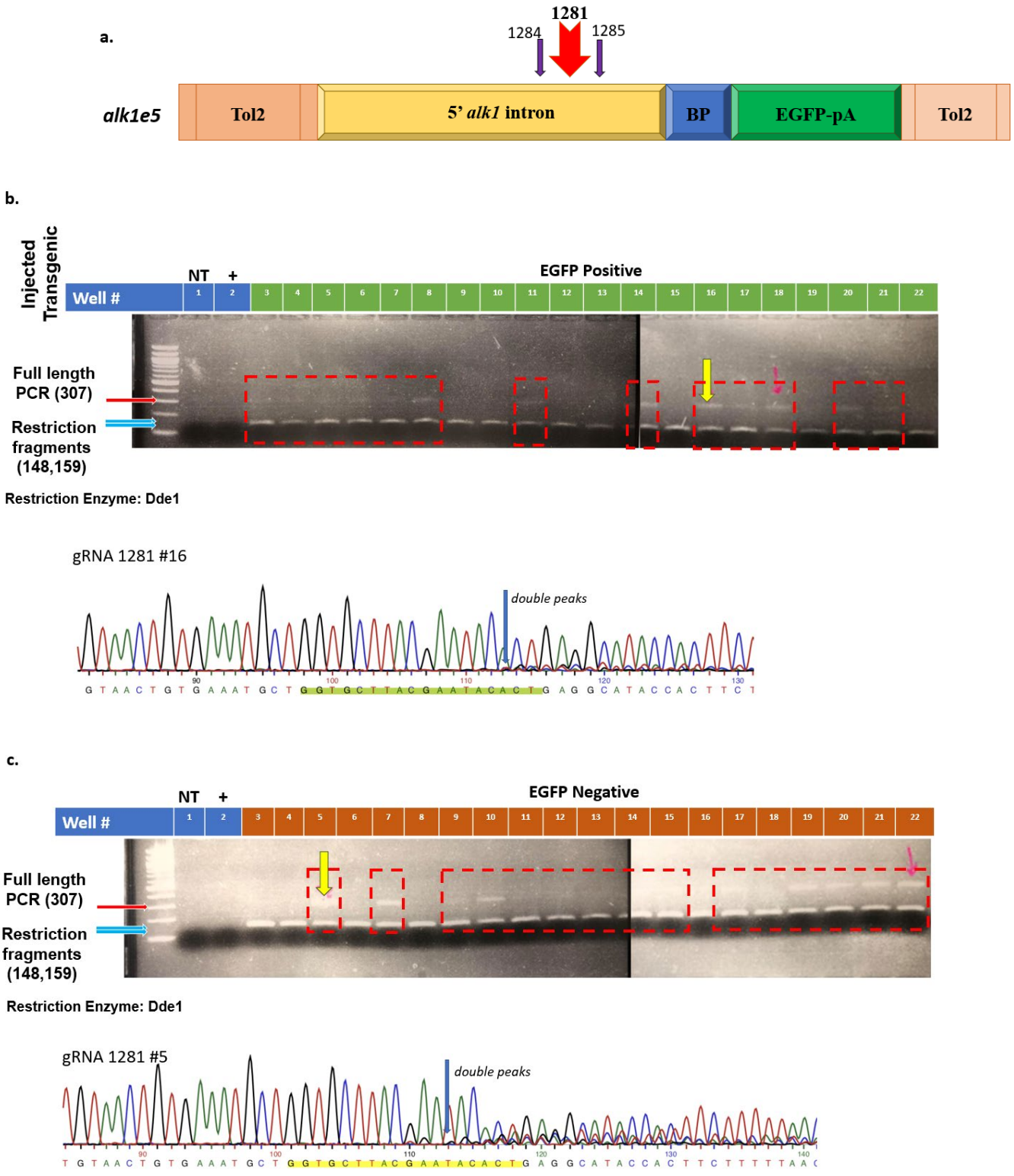

Figure 6 Validation of sgRNA 1281

a) sgRNA target site and PCR primer (1284,1285) binding sites for efficiency assays for sgRNA 1281. b,c) Efficiency assay, individual embryos from EGFP-positive (b) and EGFP-negative (c) pools. Red dashed boxes represent samples showing evidence of mutation. Yellow arrows show samples chosen for sequencing. Sequencing traces show double peaks on the 3' end of the target sequence of sgRNA 1281.

3.1.2 Conclusions

I validated that sgRNA 1280 and 1281 allowed Cas9 to generate targeted DSBs in more than 50% of injected embryos. However, the within-embryo, per-cell efficiency was very low. In order to resolve this issue, I switched to Cas9 protein instead of mRNA. Cas9 mRNA is required to be translated in the cell, so there is a delay between injection and production of an active enzyme, leading to significant mosaicism. However, Cas9 protein is functional immediately after injection (Kim, Kim, Cho, Kim, & Kim, 2014). Therefore, per-cell DSBs efficiency will most likely increase using Cas9 protein.

3.2 Specific Aim 2: Delete large regions of *alk1* intron 1 in *Tg(alk1e5:egfp)* and determine whether this element is required to drive transgene expression in the observed *alk1*-like spatiotemporal pattern.

Once I established that sgRNAs 1280 and 1281 efficiently cut at their target sites, I attempted to delete large regions of the *alk1* intron 1 by co-injecting these sgRNAs. At 3 days post-fertilization (dpf), I assessed EGFP expression in injected embryos and uninjected controls, and sorted them as EGFP-negative, EGFP-positive (normal), or EGFP-positive (ectopic or altered). Because embryos were generated from an outcross of *Tg(alk1e5:egfp)* to non-transgenic fish, I expected to see a 1:1 ratio of EGFP-positive to EGFP-negative embryos. A lower ratio of EGFP-

positive to EGFP-negative embryos might suggest that removal of *alk1* intron 1 deleted an enhancer required for transgene expression. The presence of ectopic EGFP in injected embryos might suggest that removal of *alk1* intron 1 deleted a repressor that limits EGFP expression. After scoring for EGFP expression, I digested individual embryos, then pooled groups of 24 DNA samples within each category to test for the presence of a large deletion. In injected embryos, the presence of one or more bands below the expected size of the PCR product obtained from control *Tg(alk1e5:EGFP)* embryos was interpreted as evidence of deletion and was followed up by performing the same assay on individual DNA samples from the pool. The presence of multiple bands from an individual gDNA sample suggested that cutting occurred after the one-cell stage, generating mosaic embryos. Select PCR products were then gel purified and sequenced to confirm the presence of a large deletion, and P_0 lines were generated from these injected clutches.

3.2.1 Co-injection of sgRNA 1280 and sgRNA 1281

The combination of sgRNA 1280 and 1281 was tested first since both sgRNAs had been validated independently (Figure 7a). During 3 dpf, ectopic EGFP expression was seen and recorded (Figure 7b). I then assayed for large deletions in pooled DNA from injected embryos (Figure 7c). In the uninjected control group, I detected a single band of expected size (1615 bp). In pooled sgRNA-injected embryos with normal EGFP expression, I detected multiple faint bands in each pool, including a low molecular weight band (< 500 bp) that approximated the size of the expected band after complete deletion (~300 bp). Finally, three individual embryos that showed ectopic EGFP expression each showed one or more lower bands, including a band below 500 bp.

a.

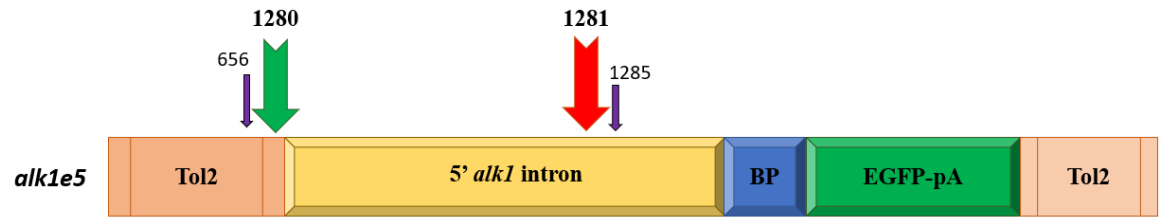

b.

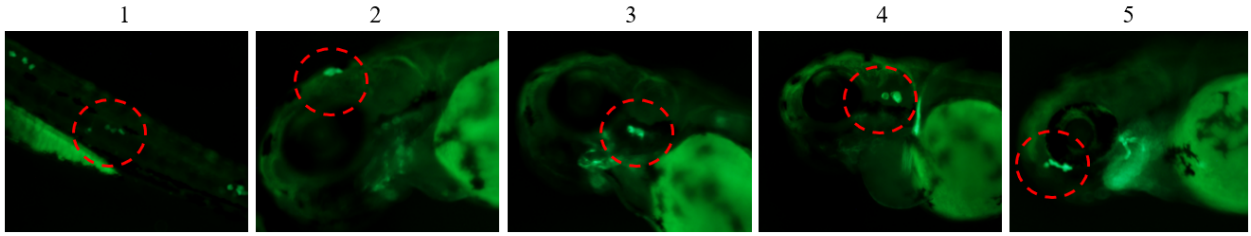

c.

Well #	1	2	3	4	5	6	7	8	9	10	11
Genomic DNA	-	pt517	E	E	E	E	E	E	E	E	E
sgRNA 1280/1	-	-	-	-	-	+	+	+	+	+	+
EGFP Expression	-	+	+	+	+	+	+	+	+	+	+

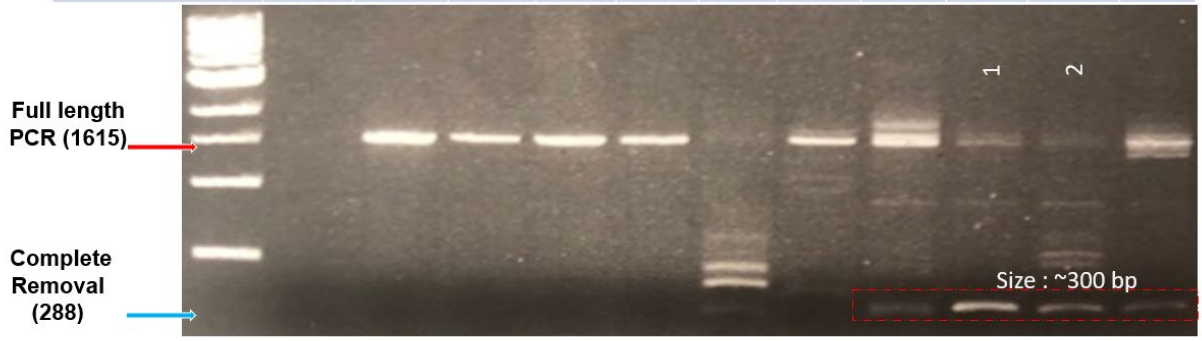

Figure 7 Validation of co-injection of sgRNA 1280 & 1281

a) sgRNA 1280 & 1281 target sites and PCR primer binding sites (656,1285) for deletion assay b) Images show examples of ectopic EGFP expression post injection. c) Results of deletion assay. Lane 2, stock *Tg(alk1e5:EGFP)*^{pt517} control gDNA. Lanes 3-5, uninjected *alk1e5:EGFP* sibling embryos. Lanes 7-8, pooled injected *alk1e5:EGFP* embryos. Lanes 9-11, individual embryos (1, 2 correspond to 1,2 in part b) that had ectopic EGFP expression. "E" is representing the Experimental DNA. Multiple bands were expected since multiple DSBs could occur independently in multiple cells, generating mosaic embryos.

After confirming the deletion of the target sequence, sgRNA 1280 and 1281 were co-injected into additional embryos. We sorted EGFP-positive embryos into two categories, EGFP-positive (normal) and EGFP-positive (ectopic) and grew these embryos to adulthood to establish a P_0 line (982g). From this line, I randomly selected four individuals from the ectopic EGFP group (potential founders A-D) and pairwise crossed them to wild type fish to generate F_1 embryos. At 3 dpf, we imaged individual EGFP-positive F_1 embryos, isolated genomic DNA from fin clips, and performed PCR to test for the targeted deletion. Of these four potential founders, only 982gA and 982gB showed evidence of transmission of a large deletion (Figure 8), whereas 982gC and 982gD did not (not shown).

Some F_1 embryos derived from 982gA had unusually strong EGFP expression, whereas others had normal EGFP expression. PCR revealed that 19/20 F1 embryos with strong EGFP expression and 6/16 F1 embryos with normal EGFP expression showed evidence of deletion, with ~700 bp PCR products instead of the full-length 1615 bp product (Figure 8b). Sequencing of select products (well numbers 1, 2, 15, 22) confirmed the same 925 bp deletion (Figure 8b, 9a,b). This allele was named pt550. Strong EGFP expression in these embryos suggests that this region of *alk1* intron 1 does not contain a critical enhancer but may in fact contain a repressor that dampens gene expression.

F_1 embryos derived from 982gB showed EGFP expression at expected ratios (data not shown). Genomic analysis of 982gB F_1 embryos revealed a large deletion in 3/27 embryos and sequencing confirmed deletion of a 1317 bp fragment (well number 58) between sgRNAs 1280 and 1281 (Figure 8c, 9a,b). This allele is pt552. However, although EGFP expression was generally low in this clutch, it was not markedly altered in these three embryos compared to their

siblings with full-length transgene. These data suggest somewhat paradoxically that the 1615 bp 5' fragment, which includes the entire pt550 deletion, is not required for transgene expression. However, further analysis is required to ensure that deletion did not significantly dampen expression.

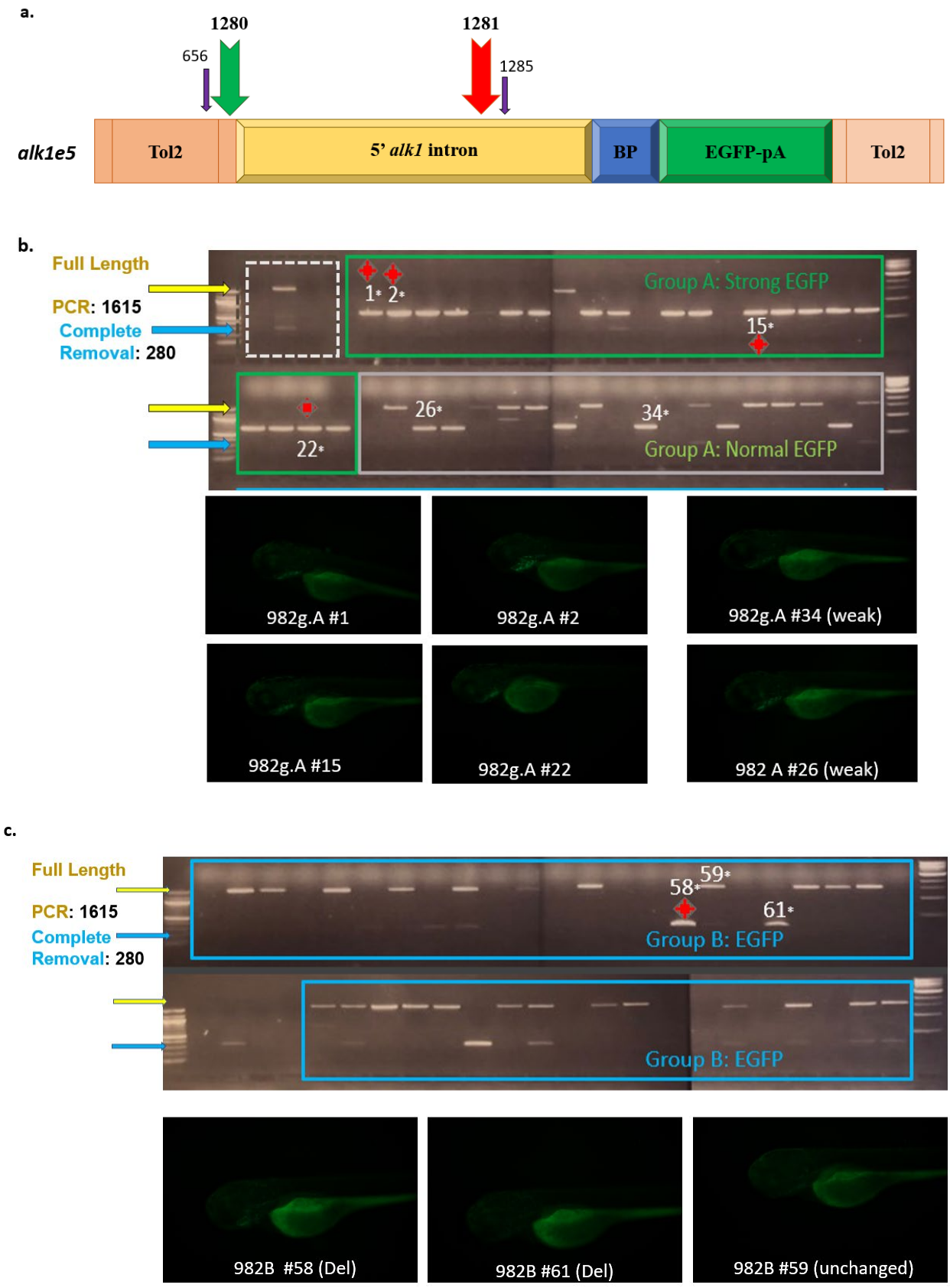

Figure 8 Identifying potential founders for sg1280/1281

a) sgRNA 1280 & 1281 target sites and PCR primer binding sites (656,1285) for deletion assay b) 1280/1281 deletion assay in F_1 offspring from 982A, with examples of embryos with strong EGFP and normal EGFP expression, below. The lanes highlighted in white are positive control (uninjected pt517 gDNA), negative control (gDNA, non-transgenic), and no template. Lanes marked with numbers and asterisks correspond to embryo images below. c) 1280/1281 deletion assay in F_1 offspring from 982B, with examples of EGFP expression below. Lanes marked with numbers and asterisks correspond to embryo images below.

a.

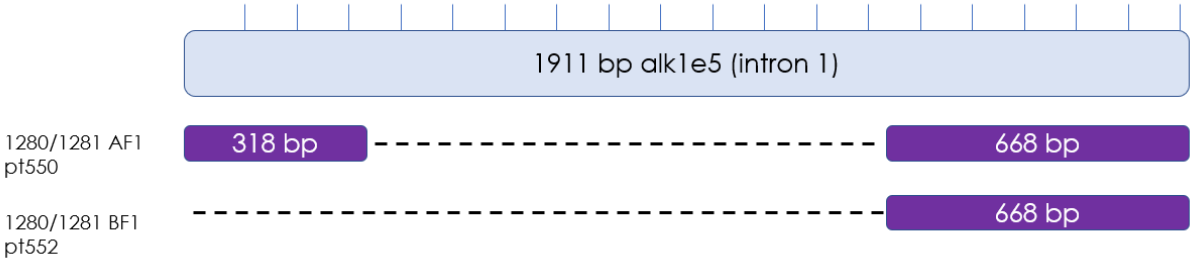
1911 bp alk1e5 (intron 1)
1280/1281 AF1 pt550
318 bp
668 bp
1280/1281 BF1 pt552
668 bp

b.

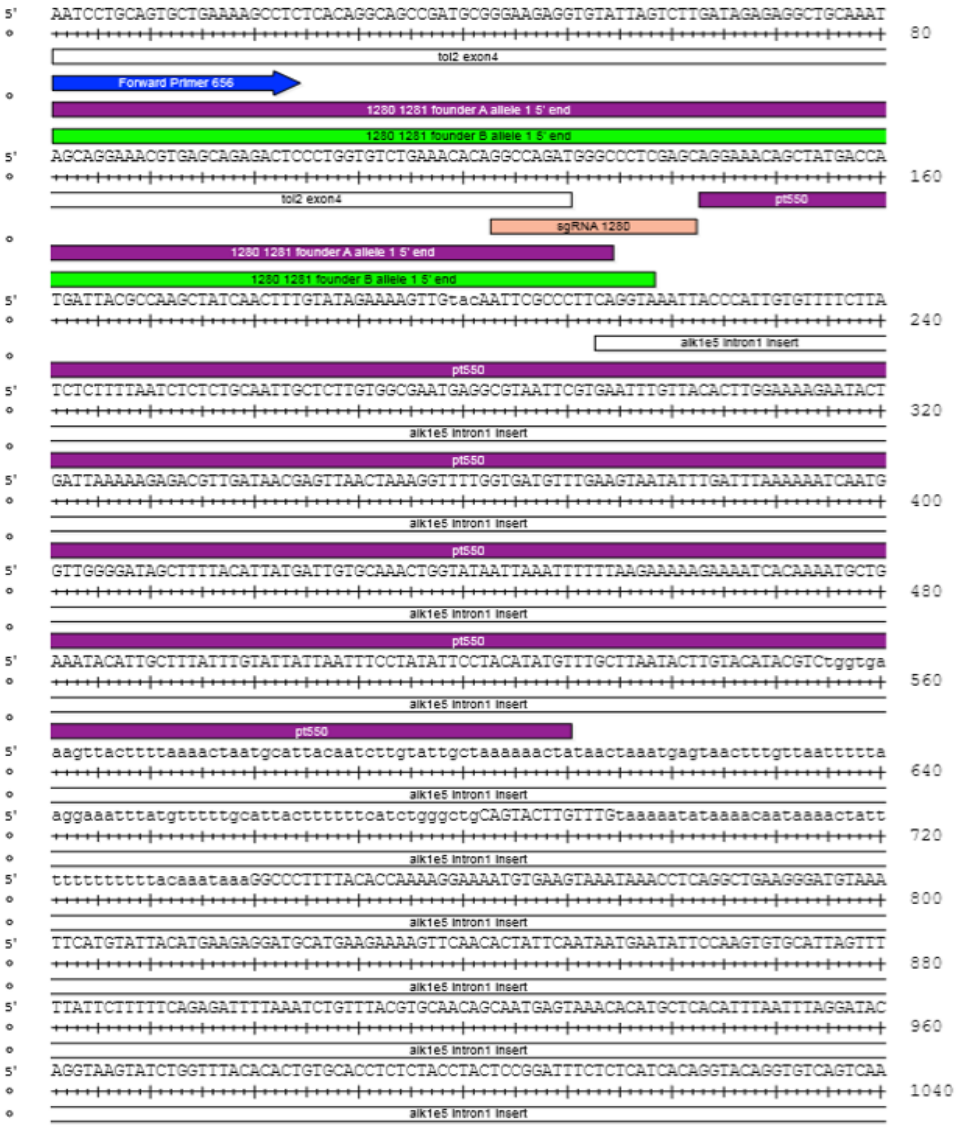
AATCCTGCAGTGCTGAAAAGCCTCTCACAGGCAGCCGATGCGGGAAGAGGTGTATTAGTCTTGATAGAGAGGCTGCAAAT
80
tol2 exon4
Forward Primer 656
1280 1281 founder A allele 1 5' end
1280 1281 founder B allele 1 5' end
AGCAGGAAACGTGAGCAGAGACTCCCTGGTGTCTGAAACACAGGCCAGATGGGCCCTCGAGCAGGAAACAGCTATGACCA
160
tol2 exon4
pt550
sgRNA 1280
1280 1281 founder A allele 1 5' end
1280 1281 founder B allele 1 5' end
TGATTACGCCAAGCTATCAACTTTGTATAGAAAAGTTGtacAATTCGCCCTTCAGGTAAATTACCCATTGTGTTTTCTTA
240
alk1e5 intron1 insert
pt550
TCTCTTTTAATCTCTCTGCAATTGCTCTTGTGGCGAATGAGGCGTAATTCGTGAATTTGTTACACTTGGAAAAGAATACT
320
alk1e5 intron1 insert
pt550
GATTAAAAAGAGACGTTGATAACGAGTTAACTAAAGGTTTTGGTGATGTTTGAAGTAATATTTGATTTAAAAAATCAATG
400
alk1e5 intron1 insert
pt550
GTTGGGGATAGCTTTTACATTATGATTGTGCAAACTGGTATAATTAAATTTTTTAAGAAAAAGAAAATCACAAAATGCTG
480
alk1e5 intron1 insert
pt550
AAATACATTGCTTTATTTGTATTATTAATTTCCTATATTCCTACATATGTTTGCTTAATACTTGTACATACGTCtggtga
560
alk1e5 intron1 insert
pt550
aagttacttttaaaactaatgcattacaatcttgtattgctaaaaaactataactaaatgagtaactttgttaatttttta
640
alk1e5 intron1 insert
aggaaatttatgtttttgcattactttttcatctgggctgCAGTACTTGTTTGtaaaaatataaaacaataaaactatt
720
alk1e5 intron1 insert
ttttttttttacaaataaaGGCCCTTTTACACCAAAAGGAAAATGTGAAGTAAATAAACCTCAGGCTGAAGGGATGTAAA
800
alk1e5 intron1 insert
TTCATGTATTACATGAAGAGGATGCATGAAGAAAAGTTCAACACTATTCAATAATGAATATTCCAAGTGTGCATTAGTTT
880
alk1e5 intron1 insert
TTATTCTTTTTCAGAGATTTTAAATCTGTTTACGTGCAACAGCAATGAGTAAACACATGCTCACATTTAATTTAGGATAC
960
alk1e5 intron1 insert
AGGTAAGTATCTGGTTTACACACTGTGCACCTCTCTACCTACTCCGGATTTCTCTCATCACAGGTACAGGTGTCAGTCAA
1040
alk1e5 intron1 insert

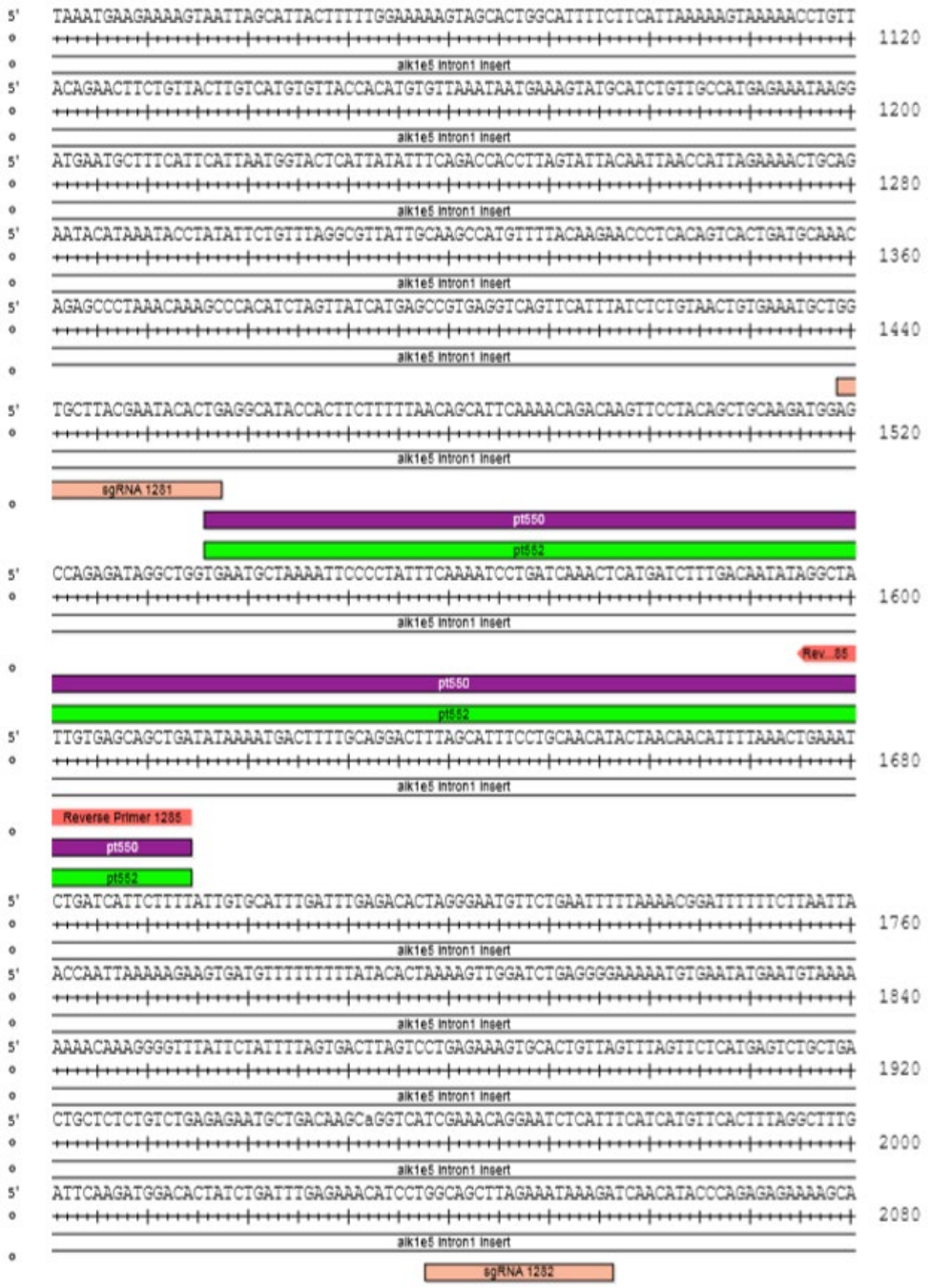

Figure 9 Sequencing results from potential founders for sg1280/1281

a) Schematic depicting deletions identified by sequencing F1 embryos from 982gA (pt550) and 982gB (pt552). b) Sequencing results depicting deletions identified by sequencing F1 embryos from 982gA (pt550) embryo #2 and 982gB (pt552) embryo #58.

3.2.2 Conclusion

Coinjection of sgRNA 1280 and 1281 was successful in deleting the targeted region of interest. Two alleles were established from two founders that transmitted the deletion to F_1 offspring. Transmission frequency is approximately 70% for founder A (pt550) and 17% for founder B (pt552). Final analysis of effects of deletion on transgene expression will require identification of F1 adults and examination of F2 offspring. However, results thus far suggest that deletion of this large intronic region does not alter transgene expression.

4.0 Discussion

Using CRISPR/Cas9, I sought to validate that the Alk1 first intron fragment within our transgenic zebrafish model, *Tg(alk1e5:egfp)*^{pt517}, is responsible for the *alk1*-like expression of EGFP. I confirmed that coinjection of sgRNAs 1280 and 1281 resulted in deletion of up to 1317 bp of the 5' end of this 1910 bp fragment. However, observation of a small number of F1 embryos did not reveal consistent effects on EGFP expression. Allele pt550, which harbors a 925 bp deletion, seemed to show increased EGFP intensity, whereas allele pt552, which harbors a 1317 bp deletion that includes the entirety of the pt550 deletion, showed no overt change in EGFP expression compared to controls. Although it is possible that the deleted region in pt550 may contain a repressor element, the fact that pt552 showed no change in EGFP does not support this hypothesis. However, very few pt552 F1 embryos were analyzed. Analysis of F2 offspring is required to gain further insight into effects of these deletions on EGFP expression. If pt552 F2 offspring show normal EGFP expression, we will conclude that the 5' end of the 1910 bp *alk1* intronic fragment is not required for the highly restricted pattern of *egfp* expression in our transgenic line.

Future experiments will focus on probing the role of the 3' end of the this intronic element in driving egfp expression, using CRISPR/Cas9-mediated genome editing. If deletion of the entire intronic fragment alters *egfp* expression, we will validate the role of this element in endogenous *alk1* expression, and examine the 3' end for critical *cis*-regulatory elements. If deletion of the entire intronic fragment does not alter egfp expression, we will conclude that it is not required for the *alk1*-like expression of EGFP and that expression pattern is dependent on local genomic regulatory elements, some of which may drive *sox7* expression.

Bibliography

Bassett, A. R., & Liu, J. L. (2014). CRISPR/Cas9 and genome editing in Drosophila. *J Genet Genomics, 41*(1), 7-19. doi:10.1016/j.jgg.2013.12.004

Begbie, M. E., Wallace, G. M., & Shovlin, C. L. (2003). Hereditary haemorrhagic telangiectasia (Osler-Weber-Rendu syndrome): a view from the 21st century. *Postgrad Med J, 79*(927), 18-24. doi:10.1136/pmj.79.927.18

Corti, P., Young, S., Chen, C. Y., Patrick, M. J., Rochon, E. R., Pekkan, K., & Roman, B. L. (2011). Interaction between alk1 and blood flow in the development of arteriovenous malformations. *Development, 138*(8), 1573-1582. doi:10.1242/dev.060467

David, L., Mallet, C., Mazerbourg, S., Feige, J. J., & Bailly, S. (2007). Identification of BMP9 and BMP10 as functional activators of the orphan activin receptor-like kinase 1 (ALK1) in endothelial cells. *Blood, 109*(5), 1953-1961. doi:10.1182/blood-2006-07-034124

Felli, E., Addeo, P., Faitot, F., Nappo, G., Oncioiu, C., & Bachellier, P. (2017). Liver transplantation for hereditary hemorrhagic telangiectasia: a systematic review. *HPB (Oxford), 19*(7), 567-572. doi:10.1016/j.hpb.2017.03.005

Gallione, C. J., Repetto, G. M., Legius, E., Rustgi, A. K., Schelley, S. L., Tejpar, S., . . . Marchuk, D. A. (2004). A combined syndrome of juvenile polyposis and hereditary haemorrhagic telangiectasia associated with mutations in MADH4 (SMAD4). *Lancet, 363*(9412), 852-859. doi:10.1016/S0140-6736(04)15732-2

Garrido-Martin, E. M., Blanco, F. J., Roque, M., Novensa, L., Tarocchi, M., Lang, U. E., . . . Bernabeu, C. (2013). Vascular injury triggers Kruppel-like factor 6 mobilization and cooperation with specificity protein 1 to promote endothelial activation through upregulation of the activin receptor-like kinase 1 gene. *Circ Res, 112*(1), 113-127. doi:10.1161/CIRCRESAHA.112.275586

Govani, F. S., & Shovlin, C. L. (2009). Hereditary haemorrhagic telangiectasia: a clinical and scientific review. *Eur J Hum Genet, 17*(7), 860-871. doi:10.1038/ejhg.2009.35

Guttmacher, A. E., Marchuk, D. A., & White, R. I., Jr. (1995). Hereditary hemorrhagic telangiectasia. *N Engl J Med, 333*(14), 918-924. doi:10.1056/NEJM199510053331407

Howe, K., Clark, M. D., Torroja, C. F., Torrance, J., Berthelot, C., Muffato, M., . . . Stemple, D. L. (2013). The zebrafish reference genome sequence and its relationship to the human genome. *Nature, 496*(7446), 498-503. doi:10.1038/nature12111

Khurshid, I., & Downie, G. H. (2002). Pulmonary arteriovenous malformation. *Postgrad Med J, 78*(918), 191-197. doi:10.1136/pmj.78.918.191

Kim, S., Kim, D., Cho, S. W., Kim, J., & Kim, J. S. (2014). Highly efficient RNA-guided genome editing in human cells via delivery of purified Cas9 ribonucleoproteins. *Genome Res, 24*(6), 1012-1019. doi:10.1101/gr.171322.113

Laux, D. W., Young, S., Donovan, J. P., Mansfield, C. J., Upton, P. D., & Roman, B. L. (2013). Circulating Bmp10 acts through endothelial Alk1 to mediate flow-dependent arterial quiescence. *Development, 140*(16), 3403-3412. doi:10.1242/dev.095307

Li, X., Yonenaga, Y., & Seki, T. (2009). Shortened ALK1 regulatory fragment maintains a specific activity in arteries feeding ischemic tissues. *Gene Ther, 16*(8), 1034-1041. doi:10.1038/gt.2009.53

Liu, J., Zhou, Y., Qi, X., Chen, J., Chen, W., Qiu, G., . . . Wu, N. (2017). CRISPR/Cas9 in zebrafish:

an efficient combination for human genetic diseases modeling. *Hum Genet, 136*(1), 1-12. doi:10.1007/s00439-016-1739-6

McDonald, J., & Pyeritz, R. E. (1993). Hereditary Hemorrhagic Telangiectasia. In M. P. Adam, H. H. Ardinger, R. A. Pagon, S. E. Wallace, L. J. H. Bean, K. Stephens, & A. Amemiya (Eds.), *GeneReviews((R))*. Seattle (WA).

Rochon, E. R., Menon, P. G., & Roman, B. L. (2016). Alk1 controls arterial endothelial cell migration in lumenized vessels. *Development, 143*(14), 2593-2602. doi:10.1242/dev.135392

Roman, B. L., & Hinck, A. P. (2017). ALK1 signaling in development and disease: new paradigms. *Cell Mol Life Sci, 74*(24), 4539-4560. doi:10.1007/s00018-017-2636-4

Roman, B. L., Pham, V. N., Lawson, N. D., Kulik, M., Childs, S., Lekven, A. C., . . . Weinstein, B. M. (2002). Disruption of acvrl1 increases endothelial cell number in zebrafish cranial vessels. *Development, 129*(12), 3009-3019. Retrieved from https://www.ncbi.nlm.nih.gov/pubmed/12050147

Ruiz-Llorente, L., Gallardo-Vara, E., Rossi, E., Smadja, D. M., Botella, L. M., & Bernabeu, C. (2017). Endoglin and alk1 as therapeutic targets for hereditary hemorrhagic telangiectasia. *Expert Opin Ther Targets, 21*(10), 933-947. doi:10.1080/14728222.2017.1365839

Seki, T., Hong, K. H., Yun, J., Kim, S. J., & Oh, S. P. (2004). Isolation of a regulatory region of activin receptor-like kinase 1 gene sufficient for arterial endothelium-specific expression. *Circ Res, 94*(8), e72-77. doi:10.1161/01.RES.0000127048.81744.31

Shovlin, C. L. (2015). Circulatory contributors to the phenotype in hereditary hemorrhagic telangiectasia. *Front Genet, 6*, 101. doi:10.3389/fgene.2015.00101

Shovlin, C. L., Hughes, J. M., Tuddenham, E. G., Temperley, I., Perembelon, Y. F., Scott, J., . . . Seidman, J. G. (1994). A gene for hereditary haemorrhagic telangiectasia maps to chromosome 9q3. *Nat Genet, 6*(2), 205-209. doi:10.1038/ng0294-205

Tillet, E., Ouarne, M., Desroches-Castan, A., Mallet, C., Subileau, M., Didier, R., . . . Bailly, S. (2018). A heterodimer formed by bone morphogenetic protein 9 (BMP9) and BMP10 provides most BMP biological activity in plasma. *J Biol Chem, 293*(28), 10963-10974. doi:10.1074/jbc.RA118.002968

Tual-Chalot, S., Mahmoud, M., Allinson, K. R., Redgrave, R. E., Zhai, Z., Oh, S. P., . . . Arthur, H. M. (2014). Endothelial depletion of Acvrl1 in mice leads to arteriovenous malformations associated with reduced endoglin expression. *PLoS One, 9*(6), e98646. doi:10.1371/journal.pone.0098646

White, R. I., Jr., Lynch-Nyhan, A., Terry, P., Buescher, P. C., Farmlett, E. J., Charnas, L., . . . Mitchell, S. E. (1988). Pulmonary arteriovenous malformations: techniques and long-term outcome of embolotherapy. *Radiology, 169*(3), 663-669. doi:10.1148/radiology.169.3.3186989

Whitehead, K. J., Smith, M. C., & Li, D. Y. (2013). Arteriovenous malformations and other vascular malformation syndromes. *Cold Spring Harb Perspect Med, 3*(2), a006635. doi:10.1101/cshperspect.a006635

Willinsky, R. A., Lasjaunias, P., Terbrugge, K., & Burrows, P. (1990). Multiple cerebral arteriovenous malformations (AVMs). Review of our experience from 203 patients with cerebral vascular lesions. *Neuroradiology, 32*(3), 207-210. Retrieved from https://www.ncbi.nlm.nih.gov/pubmed/2215905

Wooderchak-Donahue, W. L., McDonald, J., O'Fallon, B., Upton, P. D., Li, W., Roman, B. L., . . . Bayrak-Toydemir, P. (2013). BMP9 mutations cause a vascular-anomaly syndrome with phenotypic overlap with hereditary hemorrhagic telangiectasia. *Am J Hum Genet, 93*(3), 530-537. doi:10.1016/j.ajhg.2013.07.004